Vol. 39, No. 4 (2017) 471-481, DOI: 10.24874/ti.2017.39.04.06

Tribology in Industry

www.tribology.fink.rs

RESEARCH

Study of the Parametric Performance of Solid Particle Erosion Wear under the Slurry Pot Test Rig

S.R. More [a], D.V. Bhatt [a], J.V. Menghani [a]

[a] *S.V. National Institute of Technology, MED, Surat, Gujarat, India.*

Keywords:

Taguchi method
Slurry pot Test Rig
Erosion wear
SS304

Corresponding author:

Satish R. More
S.V. National Institute of Technology,
MED, Surat, Gujarat, India.
E-mail: moresatish11@yahoo.co.in

A B S T R A C T

Stainless Steel (SS) 304 is commonly used material for slurry handling applications like pipelines, valves, pumps and other equipment's. Slurry erosion wear is a common problem in many engineering applications like process industry, thermal and hydraulic power plants and slurry handling equipments. In this paper, experimental investigation of the influence of solid particle size, impact velocity, impact angle and solid concentration parameters in slurry erosion wear behavior of SS 304 using slurry pot test rig. In this study the design of experiments was considered using Taguchi technique. A comparison has been made for the experimental and Taguchi technique results. The erosion wear morphology was studied using micro-graph obtained by scanning electron microscope (SEM) analysis. At shallow impact angle 30°, the material removal pattern was observed in the form of micro displacing, scratching and ploughing with plastic deformation of the material. At 60° impact angle, mixed type of micro indentations and pitting action is observed. At normal impact angle 90°, the material removal pattern was observed in form of indentation and rounded lips. It is found that particle velocity was the most influence factor than impact angle, size and solid concentration. From this investigation, it can be concluded that the slurry erosion wear is minimized by controlling the slurry flow velocity which improves the service life of the slurry handling equipments. From the comparison of experimental and Taguchi experimental design results it is found that the percentage deviation was very small with a higher correlation coefficient (r^2) 0.987 which is agreeable.

1. INTRODUCTION

Slurry erosion wear is the mechanical degradation (loss) of any engineering material subjected to impact of a solid particle on its surface which is suspended in liquid. Slurry erosion wear resistance is a significant consideration while designing different engineering component made out of SS 304 such as slurry handling pipelines, flow control valve, blades of water and gas turbines, centrifugal pumps, waste and sewage water treatment plant and chemical industries. Based on the different applications, the researchers have invented different type of laboratory test rigs to identify the slurry erosion wear rate and material removal mechanism under the various operating conditions. They are, Miller Test Apparatus, Jet Impingement Tester [1], Falling Jet Test Apparatus [2], Jet-In-Slit Apparatus [3], Centrifugal Erosion Tester [4], Concentric Cylindrical Test Rig, Coriolis Erosion Tester [5] and Slurry Pot Tester [6]. Slurry erosion wear is a complicated phenomenon to identify the most significant parameter for erosion wear and how much its percentage. The slurry erosion wear mostly depends on solid particle velocity, impact angle, and particle size and particle concentration [6-8].

The design of the experiment is one of the best tool to identify the optimum significant parameters or factors for any process and application [9,10]. They have studied mechanical properties and erosion wear behavior of hybrid and glass fiber reinforced polyester composites material by using air jet erosion wear test rig. They observed fiber loading is the significant factor affecting the erosion wear rate than stand-off distance, impingement angle, erodent size and impact velocity. It has been found that because of increment in fiber loading, the micro hardness and strength of composite material significantly increases then erosion wear decreases. Patnaik, et al. [11-14] used air jet erosion wear test rig for investigating the significant parameters and erosion wear behavior of glass fiber polyester composites as target material with different operating parameters. They found that erodent size is the major factor affecting the erosion wear rate than fiber loading, impingement angle and impact velocity. It has been found that no such significant improvement was observed in hardness and strength with respect to fiber loading. Sahoo, et al. [15,16] investigated the effect of microstructure variations and volume fractions of primary alpha phase along with significant parameter of erosion wear on Ti-6Al-4V alloy using air jet erosion test rig. They observed impact velocity as the most significant parameter than microstructure variation. It has been found that because of percentage increment in the volume fraction of primary alpha phase, the hardness value decreased continuously leading to increment in erosion wear.

Mishra, et al. [17,18] studied the erosion wear behavior of ceramic coatings using air jet erosion test rig. They reported impact angle was the most significant affecting parameter as compared to erodent size, impact velocity, stand-off distance in the solid particle erosion wear. It has been found that because of brittle nature of coating, the erosion wear increased and maximum erosion is observed at 90° impact angle. Sahu, et al. [19] studied the erosion wear behavior in fly ash alumina coating material using air jet erosion wear test rig. They found that impact velocity was the most significant affecting parameter for erosion wear. It has been found that erosion wear increased because of the poor adhesion strength of coating due to torch input power variation. Gupta, et al. [20] used plasma sprayed coating of glass micro-spheres with Al_2O_3 particles on metal surface to study the significant parameters behavior on erosion wear using air jet test rig. They found that impact velocity is the most significant parameter than the erodent size, impingement angle, erodent temperature and alumina content parameters. It has been found that glass micro-spheres Al_2O_3 particles coating does not give significant improvement in micro-hardness with respect to borosilicate glass micro-sphere coatings because of their brittle characteristics. Paul, et al. [21] investigated the significant factor and erosion wear behavior of laser clad surface of WC reinforced Ni matrix on austenitic stainless steel with variation of Ni percentage. It has been found that impact velocity is the most significant factor affecting erosion wear. They found that there is no significant improvement in micro-hardness of Ni matrix percentage variations in coatings.

Mantry, et al. [22] applied plasma sprayed method for Cu Slag-Al composite coatings to find out the erosion wear using air jet test rig. They found that impact velocity is the most responsible affecting parameter for the solid particle erosion wear. Yogandha, et al. [23] investigated the wear behavior of nickel-based high alloy white cast iron for the mining condition using water jet erosion test rig. They identified maximum wear angle and material removal mechanism at 30°, 60° and 90° impact angle. They found that the water velocity was the most dominating parameter than the impact angle, solid concentration and PH. Goyal, et al. [24] experimentally investigated slurry erosion behavior of HVOF spray Cr_2O_3 coating on turbine steel using high-speed erosion test rig. They found that slurry erosion wear resistance of HVOF coating was better than the uncoated steel. It has been found that erosion wear decreases because of higher hardness of coating material. They also observed that rotation speed was most dominating factor in increasing erosion rate for all investigated cases. Kucuk et al. [25] investigated abrasiveness property of blast furnace slag on ceramic coatings using abrasive slurry wear test rig. They found that rotational speed was the most significant affected parameter.

The main purpose of using slurry pot test rig is to identify and simulate the actual working conditions of the slurry pipelines, control valve, pump's impeller and casing because of better accuracy in wear prediction, ease of operation, less maintenance and high volume data generation. The literature survey indicate that several researchers have used air jet erosion wear test rig for investigating the influence of parameters like erodent size, impact velocity, erodent temperature, stand-off distance, impingement angle of various materials at different operating conditions.

However, research finding related to the investigation on influence of process parameters like particle velocity, particle size, solid concentration, impact angle of slurry pot test rig is inadequate and there is a need for refined slurry erosion wear analysis. The stainless steel (SS) 304 is one of widely used wear resistance material is the most commonly used for slurry handling equipments like slurry handling pipelines, control valves, pumps and other equipment's.

Hence, the aim of the present research was to investigate the significant influence of aforesaid parameters in erosion behavior of Stainless Steel (SS) 304 using Indian Standard Sand as solid particle erodent in slurry pot test rig under various stimulated actual working conditions by considering Taguchi's experimental design.

2. EXPERIMENTAL DETAILS

2.1 Slurry Pot Test Rig

A seven liters capacity slurry pot test rig has been used for the present experimental work. The photographic view of experimental test setup with details of wear sample fixing arrangement along slurry pot and PTB propeller are shown in Fig. 1 (a). A drilling machine and two AC electric motors (1.5 HP) with variable frequency drive (VFD) are used as an accessory for the present experimental setup. One VFD is attached to drilling machine motor to control the speed of sample holding shaft which is on the top side of the pot. Another motor and VFD is attached to PTB propeller shaft which is at the bottom side of the pot. All the parts are made of SS 304 material. The four numbers of baffles are located at inner side of the pot to break the vertex flow motion developed due to the bottom propeller. At a bottom of pot 20 mm diameter size hole is provided for remove the slurry.

a)

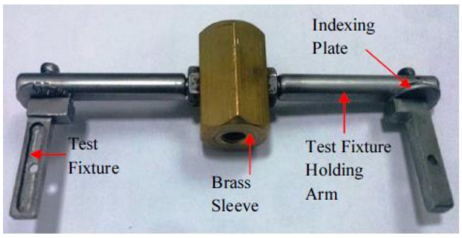

b)

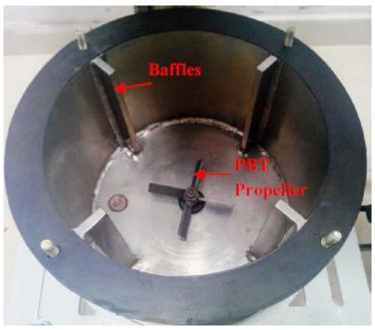

c)

Fig.1. Photograph of (a) Slurry pot test rig, (b) Fixing arrangement of wear sample and (c) Details of Pot with PTB Propeller

The test fixtures are held with two horizontal arms which are attached to brass sleeve of size 25 mm diameter and 30 mm length at the position of lower end of the top shaft. The pictorial view of test sample fixing arrangement is as shown in Fig. 1 (b). The both side rounded slot of size 30 mm length, 5 mm width and 2 mm depth was created at the test fixture to fix a test specimen inside it as shown in Fig. 1 (b). A rectangular tooth of 2.5 mm width and 1 mm thickness was created on each fixture to hold it at the necessary angle from 0° to 90° with steps of 15°, along with the direction of peripheral velocity, using the slotted angular plate as shown in Fig. 1 (b). For balancing the dynamic force and minimized wake interference effect the two test fixtures are mounted at 180° apart from each other. For controlling the rotational motion effect the test sample fixture is rotated in opposite direction to the propeller shaft at 71 mm radius. Hence, the swept volume of wear sample and holding arm is negligible.

2.2 Testing Materials and Sample Preparation

For the present investigation, SS 304 a ductile material was selected as target material for solid particle erosion wear. The elemental compositions of SS 304 were shown in Table 1. The specific gravity of SS 304 is 2.7 g/cc. The size of the wear sample used was (30 mm x 5 mm), rounded at the both ends with a thickness of 2 mm (surface are 144.64 mm^2) to fit in the slot of the test fixture as shown in Fig. 1 (b). Each test sample was fixed in the test fixture slot with the help of glue. In each experiment fresh wear sample was used, each sample was polished with #600, #1000 and #1200 emery paper for the mirror finish. The samples were cleaned with tap water and acetone after the mirror finishing operation. Finally, samples were dried using hot air dryer. This process of cleaning and drying was repeated before and after the experiment. The weight balance with least count of 0.1 mg is used to measure the test sample weight before and after the experimentation.

The correlation reported by Bree, et. al. [26] was used to compute the erosion wear rate for that average mass loss of two wear sample is considered.

$$Ew = \frac{W_L}{\rho_S \times A_{SP} \times Cv \times V_{SP} \times T \times Sin\alpha} \quad (1)$$

$$\text{Where } Cv = \frac{Cw}{\rho_S - (\rho_S - 1) \times Cw} \quad (2)$$

Cv - Solid concentration by volume in fraction; Cw - Solid concentration by weight in fraction; ρ_S - Solid particle mass density in kg/m^3; Ew - Total erosion wear rate in g/g; A_{SP} - Surface area of the wear sample subjected to erosion in m^2; T - Time over which mass loss has been measured in sec; V_{SP} - Peripheral velocity of wear specimen in m/s; W_L - Measured mass loss in kg; α - Orientation angle of wear specimen in degree.

In the present study Indian Standard (IS) Sand was used as solid particle erodent. The collection of the same size of sand particles was not possible for the IS sand therefore particles were sieved using consecutive sieve size and collection between them were designated by the mean sieve size. The different set of sieves with automatic sieve shaker was used for uniform force and shaking time for each size of particles. This sieve analysis was done with only dry sample. The physical properties of IS sand is shown in Table 2.

The collection of IS Sand particles was done from all the three grades i.e. Grade I, II and III. The mean particle size of 550 µm was collected from grade I, as the material retained between the two sieves of 500 µm and 600 µm sizes (+ 500 µm & - 600 µm). Similarly, the solid particles of size 350 µm and 150 µm were collected from grade II & III respectively. The SEM micrographs of IS sand for three different particle size namely 150 µm, 350 µm & 550 µm is shown in Fig. 2. From the SEM micrographs of IS sand, it is clear that the shape of particle irregular for all the three particle size.

Table 1. Elemental Composition of target material used.

Sr. No.	Target Material	Elemental composition (weight %)								
		C	Mn	P	S	Si	Cr	Ni	Mo	N
01	SS 304	0.020	2.10	0.047	0.034	0.71	17.50 – 19.50	8 – 13	-	0.14

Table 2. Physical Properties of IS Sand.

Sr. No.	Solid particle	Color	Chemical formula	Particle Shape	Hardness VHN	Sp. Gravity (Kg/m^3)
01	IS Sand (Quartz)	Whitish	SiO_2	Sub Angular	1100	2652

Table 3. Experimental testing parameters and their level for erosion experiments.

S.N.	**Erosion parameters**	**Units / Symbols**	**Level**		
			1	**2**	**3**
1	Particle Velocity (V)	Meter per sec (m/s)	4	6	8
2	Slurry Concentration (C)	Percent by weight (%)	10	20	30
3	Angle of Impingement (A)	Degree (°)	30	60	90
4	Particle Size (S)	Micron (μm)	150	350	550

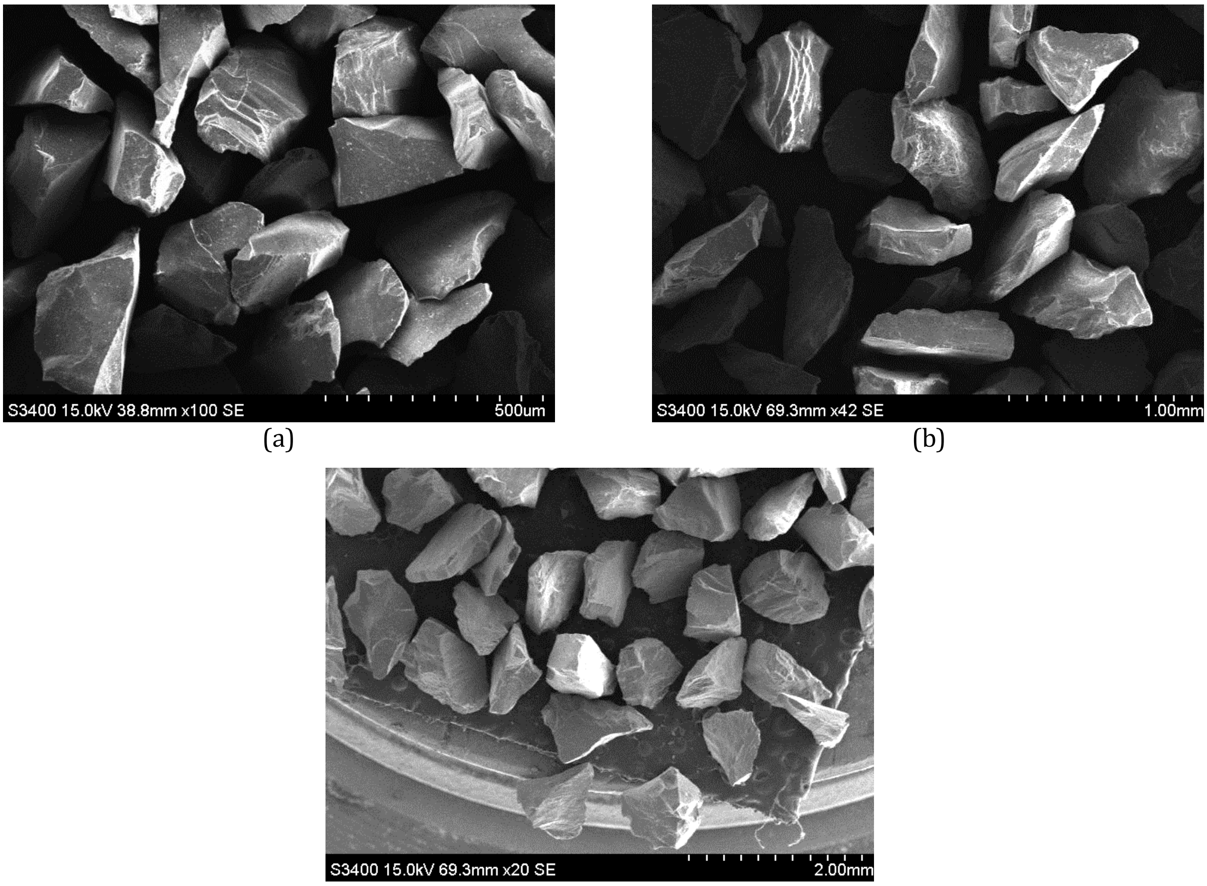

Fig. 2. SEM of Erodent (IS Sand) (a) 150 μm, (b) 350 μm, (c) 550 μm.

2.3 Experimental Design

Taguchi's design of experiments technique was used for analyzing the significant influence of control parameters and development of a model on the performance output. Using this method, the effect of each single condition can be easily studied. In slurry erosion wear process, the output wear rate depends on the number of input parameters. Taguchi's design of experiments was considered because it is more flexible rather than other analytical techniques in identifying the influence of each input parameters on erosion wear rate. The Taguchi's design of experiment approach L9 was considered because it reduces the experimental cost and time.

In this study, four parameters namely impact angle, impact velocity, solid concentration and solid particle size were considered in order to study rate of erosion wear response of AISI SS 304. In all the experiments, the testing parameters and levels used were shown in Table 3. The operating conditions for each test were shown in Table 4. The experimental results were transformed into a signal-to-noise (S/N) ratio.

There are various S/N ratios existing depending on the type of characteristic; that is, smaller the better, nominal the best, and larger the better. The smaller the better characteristic of S/N ratio was considered for studying the minimum erosion wear rate as shown in equation 3.

The smaller the better characteristic:

$$\frac{S}{N} = -10\log\frac{1}{n}\left(\sum y^2\right) \qquad (3)$$

where, n is the number of observations and y is the observed data i.e. erosion wear rate or mass loss Patnaik, et al. [11-13].

3. RESULT AND DISCUSSIONS

3.1 Erosion Wear Analysis Using Taguchi Experimental Design

The MINITAB 14 software package was used for the present experiment analysis. The L9 orthogonal array design along with S/N ratio for the analysis of erosion wear rate experimental results were shown in Table 4. Lower the better quality characteristic was selected to obtain the optimal possible parameters for the erosion wear rate.

The response table for the S/N ratio obtained is presented in Table 5. Solid particle impact velocity was the most influencing significant control parameter among all four factors for causing the solid particle erosion wear rate of SS 304 as shown in Table 5. The remaining three parameters i.e. angle of impact, slurry concentration, and particle size is ranked second, third and fourth respectively in influencing solid particle erosion on SS 304.

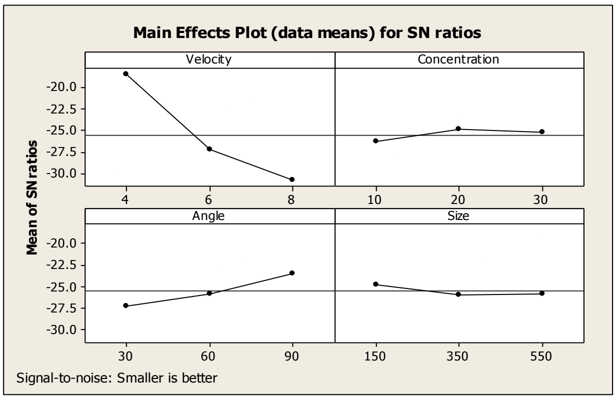

Fig. 3. Main effects plot for S/N ratios.

The graphical results of main effect plot for the S/N rations were represented in Fig. 3. The (mass loss) solid particle erosion of SS 304 was found to be lower in the 4 m/s velocity followed by the 6 m/s and 8 m/s. At 90° impact angle minimum erosion wear rate is obtained as compared to 60° and 30° impact angle. At 20 % solid concentration minimum erosion wear rate was found as compare to 10 % and 30 % by weight solid concentration. Therefore, it is found that solid particle erosion wear rate on SS 304 was less influenced by solid particle concentration.

Table 4. Taguchi's L9 experimental results of erosion test and their S/N Rations.

Exp. No.	Particle Velocity (V), m/s	Slurry Concentration (C), %	Angle of Impingement (A), °	Particle Size (S), µm	Erosion Wear Rate (Ew), gm/gm (x10^{-8})	S/N Ratio (dB)
1	4	10	30	150	10.3631	-20.3098
2	4	20	60	350	8.6223	-18.7125
3	4	30	90	550	6.6429	-16.4472
4	6	10	60	550	27.5406	-28.7995
5	6	20	90	150	15.5861	-23.8547
6	6	30	30	350	28.8469	-29.202
7	8	10	90	350	31.5042	-29.9674
8	8	20	30	550	40.6136	-32.1734
9	8	30	60	150	32.1128	-30.1336

Table 5. S/N ratio Response table using the characteristics of smaller the better.

Level	Particle Velocity (A)	Slurry Conc. (B)	Angle of Impact (C)	Particle Size (D)
I	-18.49	-26.36	-27.23	-24.77
II	-27.29	-24.91	-25.88	-25.96
III	-30.76	-25.26	-23.42	-25.81
Delta	12.27	1.45	3.81	1.19
Rank	1	3	2	4

3.2. Surface Morphology Using SEM

The surfaces of the eroded samples of a) 150μm b) 350μm c) 550μm particle size were analyzed for 30°, 60° and 90° degree impact angles under a scanning electron microscope (SEM) as shown in Fig. 4 to 6 respectively. The harsh ploughing marks were also largely observed on the wear surfaces of the sample. The different type of material removal mechanisms like large pile-up or ploughing, crates, leading to the formation of platelet (flake), cutting action, lip fragmentation and indentations are responsible in solid particle erosion of SS 304 [8,15,23-25].

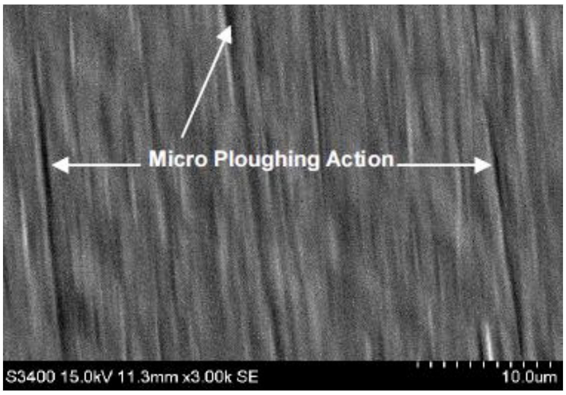

(a)

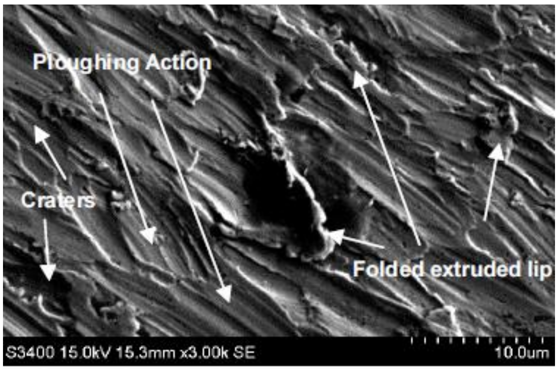

(b)

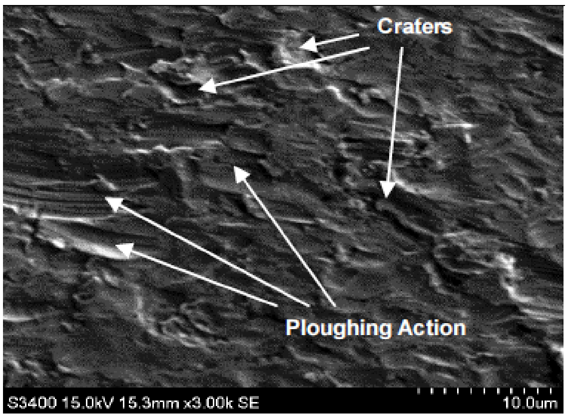

(c)

Fig. 4. Surface morphology (SEM) at 30° angle of impact and particle size (a) 150 μm, (b) 350 μm, (c) 550 μm.

The material removal mechanism mostly depends on the sample surface properties and the impact angle of a solid particle on the surface of wear substrate [24]. The surface topography/morphologies at 30° lower impact angle were shown in Fig. 4 (a-c). At 30° impact angle it is observed that the material removal by deep ploughing mechanism followed by micro fracture as shown in Fig. 4 (a-c). At 30° impact angle, maximum erosion occurrence takes place due to maximum cutting velocity component than the deformation velocity leading to ploughing and scattering of the particles [8,15].

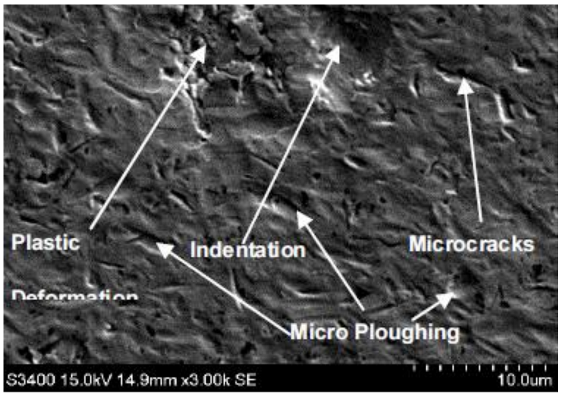

(a)

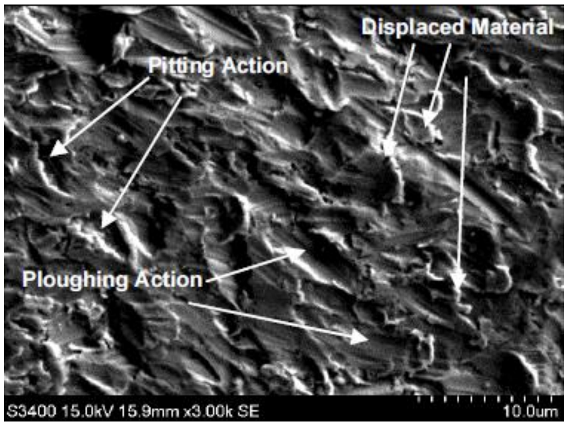

(b)

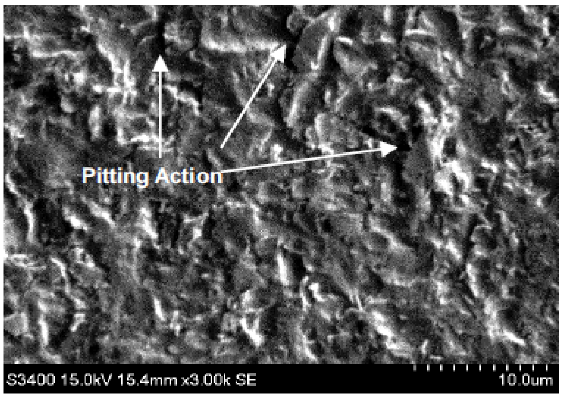

(c)

Fig. 5. Surface morphology (SEM) at 60° angle of impact and particle size (a) 150μm, (b) 350μm, (c) 550μm.

The surface topography/morphologies at 60° impact angle were shown in Fig. 5 (a-c). At 60° impact angle it is observed that the mixed type of material removal mechanism takes place. At 60° impact angle the micro ploughing, cutting action and large chips forming leads to consequently removal of the material from the sample surface [8,23].

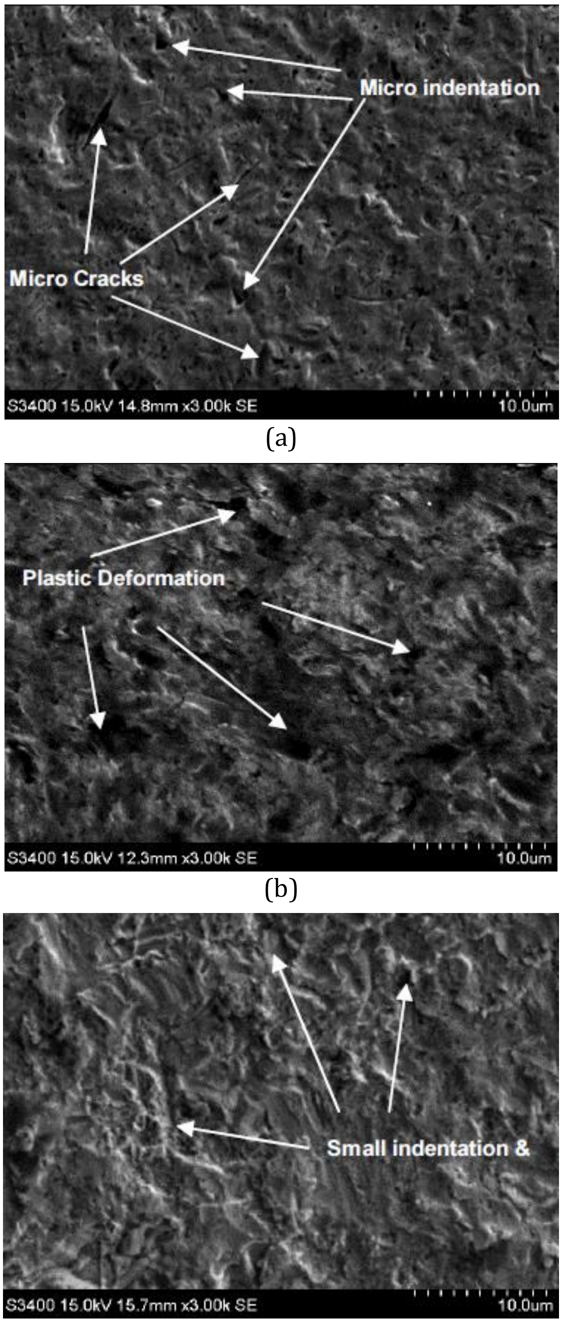

Fig. 6. Surface morphology (SEM) at 90° angle of impact and particle size (a) 150 μm, (b) 350 μm, (c) 550 μm.

The surface topography/morphologies at 90° impact angle were shown in Fig. 6 (a-c). At the 90° impact angle the large and deep indentation, protruded lips and craters were formed as shown in Fig. 6 (a-c). These protruded lips are removed by repeated impact of the solid particles [8,25]. At this impact angle it is found that the material is displaced by plastic deformation around the crater and forms a rim i.e. rounded indentation craters because of repetitive impact of solid particles. The long platelet ploughing types craters (smear type crater) will disappear which are replaced by indentation craters as shown in Fig. 6 (a-c). At this impact angle it is also observed that due to the further impact of the particles, the rim gets flattened and fracture takes place [8,24]. Therefore less material loss was observed at this impact angle as compared to other impact angles.

3.3. Erosion Wear Rate Prediction Using Predictive Equation

The erosion wear rate due to solid particle was predicted using the nonlinear regressive predictive equation for showing the relationship between the erosion wear and combination of control parameters. This regression study was done by using Datafit 9.1.32 & Minitab 14 software is used. The following form of the regression equation was obtained:

$$E_w = -e + (a \times V) - (b \times C) - (c \times A) + (d \times S) \quad (4)$$

where Ew - rate of erosion wear; e, a, b, c and d are the constant; V - particle velocity; C - solid concentration; A - Impact angle; S - particle size.

The values of all constants were calculated by using the Datafit 9.1 & Minitab 14 software and by using these values in equation (4) the final nonlinear regression model was obtained as follows.

$$E_w = -12.5 + (6.55 \times V) - (0.0301 \times C) - (0.145 \times A) + (0.0139 \times S) \quad (5)$$

The accuracy of calculated constants was confirmed because high correlation coefficient (r^2) of 0.987 was obtained from equation (5). The comparison between the erosion wear obtained from experimental results and predictive equation is shown in Table 6.

Table 6. Compression of experimental and predictive values for erosion wear rate.

Exp. No.	Result Obtained from Experiments	Results Obtained from Predictive Equation	Percentage Error (%)
01	10.36	11.18	7.93
02	8.62	9.32	8.15
03	6.64	7.46	12.38
04	27.54	25.51	7.35
05	15.58	15.28	1.91
06	28.84	26.47	8.22
07	31.50	31.47	0.08
08	40.61	42.66	5.04
09	32.11	32.43	1.00

Table 7. Confirmation experimental results for erosion wear of SS 304.

Particle velocity (V)	Solid concentration (C)	Impact angle (A)	Particle size (S)	Erosion Rate in Test	Erosion Rate by Model	% Error
4	20	90	150	2.312	2.133	8.39

3.4. Confirmation Test

The confirmation test was performed on SS 304 by considering optimal test parameters i.e. particle velocity V_1, solid concentration C_3, impact angle A_3, and particle size S_1 at which the solid particle slurry erosion is minimum. The erosion wear rate obtained in SS 304 material due to slurry erosion using both nonlinear regression equation and confirmation experimental results are shown in Table 7. By comparing the experimental and analytical results a deviation of about 8.39 % was found which is agreeable. Therefore, it is shown that the derived nonlinear regression equation describes the slurry erosion wear rate of this material with various control factors with a reasonable degree of approximation.

4. CONCLUSIONS

The experimental results of the parametric influence of significant factor on the solid particle erosion wear behavior of SS 304 under slurry pot test rig lead to the following conclusions.

- From all the four factors, impact velocity is a most influencing significant factor of solid particle erosion wear of SS 304, followed by impact angle, solid particle size and solid concentration respectively.
- Maximum erosion wear rate took place at an impact angle of 30° showing ductile type response of the metal SS 304 to solid particle erosion wear.
- The surface morphology of eroded surface at various impact angles were observed under SEM. At 90° impact angle, deep indentation and plastic deformation type of material removal mechanism are observed. Similarly, at 30° impact angle, large ploughing action with craters is observed and at 60° mixed type of micro indentations, cracks and pitting action is observed.
- The deviation in percentage between predicted and experimental result was between 0 to 12%. A higher correlation coefficient value of (r^2) is 0.987 shows the correctness of the mathematical model used. So, the model is more suitable for further study.
- From this investigation, it can be concluded that the slurry erosion wear is minimized by controlling the slurry flow velocity which improves the service life of the slurry handling equipments.

Acknowledgments

The authors gratefully acknowledge the financial support of this research program under Approval Note No.121.MED/Institute Annual Grant provided by the Mechanical Engineering Department, SVNIT, Surat, Gujarat, India.

REFERENCES

[1] J.B. Zu, I.M. Ihtchings and G.T. Burstein, 'Design of a slurry erosion test rig', *Wear*, vol. 140, no. 2, pp. 331-344, 1990.

[2] F.Y. Lin and H.S. Shao, 'Effect of impact velocity on slurry erosion and a new design of a slurry erosion tester', *Wear*, vol. 143, no. 2, pp. 231-240, 1991.

[3] H.X. Zhao, A. Yabuki, M. Matsumura, T. Takahashi and M. Yamamoto, 'Slurry erosion properties of ceramic coatings', *Wear*, vol. 233-235, pp. 608-614, 1999.

[4] N. Hayashi, Y. Kagimoto, A. Notomi, Y. Takeda and K. Kato, 'Development of new testing method by centrifugal erosion tester at elevated temperature', *Wear*, vol. 258, no. 1-4, pp. 443-457, 2005.

[5] H.M. Hawthorne, Y. Xie and S.K. Yick, 'A new coriolis slurry erosion tester design for improved slurry dynamics', *Wear*, vol. 255, no. 1-6, pp. 170-180, 2003.

[6] G.R. Desale, B.K. Gandhi and S.C. Jain, 'Improvement in the design of a pot tester to simulate erosion wear due to solid–liquid mixture', *Wear*, vol. 259, no. 1-6, pp. 196–202, 2005.

[7] A.A. Gadhikar, A. Sharma, D.B. Goel, and C.P. Sharma, 'Fabrication and Testing of Slurry Pot Erosion Tester', *Transactions of the Indian Institute of Metals*, vol. 64, no. 4-5, pp. 493–500, 2011.

[8] S.R. More, B.D. Nandre and G.R. Desale, 'Development of Pot Tester to Simulate the Erosion Wear due to Solid-Liquid Mixture', *International Journal of Researchers, Scientists and Developers*, vol. 2, no. 1, pp. 6-12, 2014.

[9] S.S. Mahapatra, A. Patnaik and A. Satapathy, 'Taguchi method applied to parametric appraisal of erosion behavior of GF-reinforced polyester composites' *Wear*, vol. 265, pp. 214–222, 2008.

[10] S.S. Mahapatra and A. Patnaik, 'Study on mechanical and erosion wear behavior of hybrid composites using Taguchi experimental design', *Materials and Design*, vol. 30, pp. 2791–2801, 2009.

[11] A. Patnaik, 'Implementation of Taguchi Design for Erosion of Fiber-Reinforced Polyester Composite Systems with SiC Filler', *Journal of Reinforced Plastics and Composites*, vol. 27, no. 10, pp. 1-19, 2008.

[12] A. Patnaik, A. Satapathy, S.S. Mahapatra and R.R. Dash, 'A modeling approach for prediction of erosion behavior of glass fiber–polyester composites', *Journal of Polymer Research*, vol. 15, pp. 147–160, 2008.

[13] A. Patnaik, 'A Taguchi Approach for Investigation of Erosion of Glass Fiber – Polyester Composites', *Journal of Reinforced Plastics and Composites*, vol. 27, no. 8, pp. 1-18, 2008.

[14] A. Patnaik and A. Satapathy, 'Erosion Wear Response of Flyash-Glass Fiber-Polyester Composites: A Study using Taguchi Experimental Design', *Malaysian Polymer Journal*, vol. 4, no 2, pp. 13-28, 2009.

[15] R. Sahoo, S. Mantry, T.K. Sahoo, S. Mishra and B.B. Jha, 'Effect of Microstructural Variation on Erosion Wear Behavior of Ti-6Al-4V Alloy', *Tribology Transactions*, vol. 56, pp. 555-560, 2013.

[16] R. Sahoo, B.B. Jha, T.K. Sahoo and S. Mantry, 'Effect of Volume Fraction of Primary Alpha Phase on Solid Particle Erosion Behavior of Ti-6Al-4V Alloy', *Tribology Transactions*, vol. 58, pp. 1105-1118, 2015.

[17] S.C. Mishra, S. Das, A. Satapathy, P.V. Ananthapadmanabhan and K.P. Sreekumar, 'Erosion Wear Analysis of Plasma Sprayed Ceramic Coating Using the Taguchi Technique, *Tribology Transactions*, vol. 52, pp. 401-404, 2009.

[18] S.C. Mishra, S. Praharaj and A. Satpathy, 'Evaluation of Erosion Wear of A Ceramic Coating with Taguchi Approach', *Journal of Manufacturing Engineering*, vol. 4, no. 2, pp. 241-246, 2009.

[19] S.P. Sahu, A. Satapathy, A. Patnaik, K.P. Sreekumar and P.V. Ananthapadmanabhan, 'Development characterization and erosion wear response of plasma sprayed fly ash–aluminum coatings', *Materials and Design*, vol. 31, pp. 1165–1173, 2010.

[20] G. Gupta and A. Satapathy, 'Studies on Erosion Behavior of Plasma Sprayed Coatings of Glass Microspheres Premixed with Al2O3 Particles', *Advances in Tribology*, vol. 2014, p. 11, 2014. http://dx.doi.org/10.1155/2014/763601.

[21] C.P. Paul, S.K. Mishra, P. Tiwari and L.M. Kukreja, 'Solid-Particle Erosion Behaviour of WC/Ni Composite Clad layers with Different Contents of WC Particles', *Optics & Laser Technology*, vol. 50, pp. 155–162, 2013.

[22] S. Mantry, D. Behera, S.K. Mishra, D. Debasish, B.B. Jha and B.K. Mishra, 'Erosive Wear Analysis of Plasma-Sprayed Cu Slag–Al Composite Coatings', *Tribology Transactions*, vol. 56, pp. 196-202, 2013.

[23] J. Yoganandh, S. Natarajan and S.P. Kumaresh Babu, 'Erosive Wear Behavior of Nickel-Based High Alloy White Cast Iron Under Mining Conditions Using Orthogonal Array', *Journal of Materials Engineering and Performance*, vol. 22, pp. 2534–2541, 2013.

[24] D. Goyal, H. Singh, Harmesh Kumar and V. Sahni, 'Slurry Erosive Wear Evaluation of HVOF-Spray Cr2O3 Coating on Some Turbine Steels', *Journal*

of Thermal Spray Technology, vol. 21, pp. 838–851, 2012.

[25] Y. Kucuk, 'Investigation of Abrasiveness Property of Blast Furnace Slag on Ceramic Coatings via the Abrasive Slurry Wear Method', *Tribology Transactions*, vol. 55, pp. 762-771, 2012.

[26] S.E.M.De. Bree, W.F. Rosenbrand and A.W.J.de. Gee, 'On the erosion resistance in water-sand mixtures of steels for application in slurry pipelines', *Hydro transport 8, BHRA Fluid Engineering,* Johannesburg, (S.A.), Paper C3 1982.